

## Abstract

Although modern physics experiments have shown unprecedented levels of accuracy and agreement with the standard model, questions of matter over antimatter as a result of the early universe, the production of life-dependent elements from supernova bursts, as well as the process of proton decay remain at the forefront of particle physics. The DUNE physics program is a global collaboration which is focussing on answering these questions, and ultimately pushing for the solidification of grand unified theories. In this report, we provide a brief introduction to neutrino physics, particularly with respect to the three flavour neutrino oscillation paradigm, and provide a holistic view on the critical components of the DUNE physics program. While a large focus of this report is placed on the far detector modules, we include a brief discussion on the near detector, which is of central importance in maximizing the accuracy of the reconstruction of events.

# 1 Neutrino Physics

## 1.1 Neutrino Oscillations

A neutrino is an incredibly lightweight, electrically neutral subatomic particle, making it extremely challenging to experimentally study their behaviour; they interact almost exclusively with matter via weak nuclear and gravitational forces. Weak interaction is the interaction between subatomic particles which is responsible for the radioactive decay of particles, and is by extension therefore responsible for the creation of neutrinos. These neutrally charged particles have mass of magnitude so small were long thought to be massless. It has since been shown experimentally, with theoretical support provided by the Standard Model and grand unified theories, that each of these particles has their own discrete, non-zero mass.

Neutrino oscillations are a phenomenon in which a neutrino which was initially associated with a specific leptonic flavour can later be measured to have a different leptonic flavour. Under weak particle interactions, three flavours of neutrinos are created: electron neutrinos ( $\nu_e$ ), muon neutrinos ( $\nu_\mu$ ), and tau neutrinos ( $\nu_\tau$ ), each associated with the corresponding charged leptons, the electron ( $e^-$ ), the muon ( $\mu^-$ ), and the tau ( $\tau^-$ ) respectively. At any given time, a neutrino propagating through matter has an associated discrete probability distribution which encodes the probability of the neutrino being allocated to one of the three known states. These neutrino oscillations imply non-zero neutrino masses, the ordering of such, as well as the mechanism behind the non-zero masses remains one of the unsolved mysteries of particle physics [1]. The neutrino mass eigenstates  $\nu_1, \nu_2$  and  $\nu_3$ , each with mass  $m_1, m_2$  and  $m_3$  respectively act as basis for the space of neutrinos, of which appropriate linear combinations can be taken to form the (distinct) neutrino charged current interaction eigenstates (i.e. the three flavours  $\nu_e, \nu_\mu$  and  $\nu_\tau$ ) [4]. This linear combination can be unambiguously defined by the  $3 \times 3$  unitary mixing matrix, commonly referred to as the PMNS matrix:

$$\begin{pmatrix} \nu_e \\ \nu_\mu \\ \nu_\tau \end{pmatrix} = \underbrace{\begin{pmatrix} U_{e1} & U_{e2} & U_{e3} \\ U_{\mu 1} & U_{\mu 2} & U_{\mu 3} \\ U_{\tau 1} & U_{\tau 2} & U_{\tau 3} \end{pmatrix}}_{\text{PMNS}} \begin{pmatrix} \nu_1 \\ \nu_2 \\ \nu_3 \end{pmatrix} \quad (1)$$

Having some of the off-diagonal entries being non-zero, along with the distinct values of the eigenstate masses  $m_i$  results in neutrino oscillations. It has been experimentally shown that the oscillation probability is proportional to the difference of squares of the masses  $\Delta m_{ij}^2 = m_i^2 - m_j^2$ . In general, the space of  $3 \times 3$  unitary matrices is nine dimensional [1]. In the case of the PMNS matrix, five of these degrees are absorbed into phases of lepton fields. As a result, we can uniquely parameterize the PMNS matrix through the three mixing angles  $\theta_{12}, \theta_{13}$  and  $\theta_{23}$ , as well as the single phase angle  $\delta_{CP}$  which quantifies the charge parity violations. In this case, the PMNS matrix can then be decomposed into the product of three rotation matrices about each axis:

$$\underbrace{\begin{pmatrix} U_{e1} & U_{e2} & U_{e3} \\ U_{\mu 1} & U_{\mu 2} & U_{\mu 3} \\ U_{\tau 1} & U_{\tau 2} & U_{\tau 3} \end{pmatrix}}_{\substack{\text{Atmospheric Neutrinos} \\ \nu_\mu \longleftrightarrow \nu_\tau}} = \underbrace{\begin{pmatrix} 1 & 0 & 0 \\ 0 & c_{23} & s_{23} \\ 0 & -s_{23} & c_{23} \end{pmatrix}}_{\substack{\text{Reactor/Accelerator Neutrinos} \\ \nu_\mu \longleftrightarrow \nu_e}} \underbrace{\begin{pmatrix} c_{13} & 0 & s_{13}e^{-i\delta} \\ 0 & 1 & 0 \\ -s_{13}e^{i\delta} & 0 & c_{13} \end{pmatrix}}_{\substack{\text{Solar Neutrinos} \\ \nu_e \longleftrightarrow \nu_X}} \underbrace{\begin{pmatrix} c_{12} & s_{12} & 0 \\ -s_{12} & c_{12} & 0 \\ 0 & 0 & 1 \end{pmatrix}}_{\substack{\text{Solar Neutrinos} \\ \nu_e \longleftrightarrow \nu_X}} \quad (2)$$

where  $c_{ij} = \cos(\theta_{ij})$ ,  $s_{ij} = \sin(\theta_{ij})$ . It follows by convention that the mixing angles are defined as

$$\sin^2(\theta_{12}) = \frac{|U_{e2}|^2}{1 - |U_{e3}|^2} \quad \sin^2(\theta_{23}) = \frac{|U_{\mu 3}|^2}{1 - |U_{e3}|^2} \quad \sin^2(\theta_{13}) = |U_{e3}|^2 \quad (3)$$

and the complex single phase angle is given by

$$\delta_{CP} = -\arg(U_{e3}) \quad (4)$$

For  $\delta_{CP}$  non-integer multiples of  $\pi$  indicates violation of charge parity symmetry in the neutrino oscillation [1]. Note that the CP of a neutrino  $\nu$  is symmetric if all observables remain invariant under exchange with its corresponding anti-neutrino  $\bar{\nu}$ . CP violations are then naturally measured by testing the following equality;

$$P(\nu_\alpha \rightarrow \nu_\beta) = P(\bar{\nu}_\alpha \rightarrow \bar{\nu}_\beta) \quad \alpha, \beta = e, \mu, \tau, \quad \alpha \neq \beta \quad (5)$$

The propagation of the eigenstates  $\nu_j$  are described by plane waves which take the form

$$\nu_j(t) = e^{-i(E_j t - \vec{p}_j \cdot \vec{x})} \nu_j(0) \quad (6)$$

which can similarly be expressed in terms of the distance travelled  $L$  as

$$\nu_j(L) = e^{-i\left(\frac{m_j^2 L}{2E}\right)} \nu_j(0) \quad (7)$$

The oscillation probability can therefore be given by  $P_{\alpha \rightarrow \beta} = |\langle \nu_\beta, \nu_\alpha(L) \rangle|^2$  for  $\alpha, \beta = e, \mu, \tau$ , which can alternatively be expressed in terms of the elements of the PMNS matrix and the eigenstates  $\nu_j$  via (1). Expressing  $P_{\alpha \rightarrow \beta}$  in terms of the entries of the PMNS matrix reveals that the value of charge parity single phase angle  $\delta_{CP}$  affects both the amplitude and phase of the oscillation probability distribution.

## 1.2 Tau Neutrinos

Tau neutrinos  $\nu_\tau$  are particularly difficult to select and detect since their appearance is kinematically forbidden at typical beam energy levels. Further, the associated  $\tau$ -leptons have many decay modes which can mimic either  $\nu_e$  and  $\nu_\mu$  charged current events, or replicate neutral current events;  $\nu_\tau$  charged current interactions have the same particle content as  $\nu_e$  and  $\nu_\mu$  charged current events, or neutral current events [2]. Due to these inherent obstructions, it is predicted that approximately 800 tau neutrino events can be observed per year in the high-energy neutrino regime. It follows from 1 that the oscillation probability of  $\nu_\mu \rightarrow \nu_\tau$  is given by

$$P(\nu_\mu \rightarrow \nu_\tau) = \sin^2(2\theta_{23}) \sin^2\left(\frac{\Delta m_{23}^2 L}{4E}\right) \quad (8)$$

Due to the close proximity of the near detector to the source beam which produces non- $\nu_\tau$  particles, it is expected that almost zero  $\nu_\tau$  charged current events will be observed. In particular, the oscillation probability of an initially  $\nu_\mu$  flavoured neutrino transitioning to the  $\nu_\tau$  flavour is given by

$$P(\nu_\mu \rightarrow \nu_\tau) = \sin^2(2\theta_{23}) \sin^2 \frac{\Delta m_{41}^2 L}{4E} \quad (9)$$

where  $\Delta m_{41}^2$  is the mass difference of a new mass eigenstate in the  $3 + 1$  scenario [2]. This process is referred to as short-baseline sterile-driven  $\nu_\tau$  appearance. In summary, the high-energy beam mode will provide opportunities to observe  $\nu_\tau$  charged current appearance in the near detector and  $\nu_\tau$  charged current cross sections in the far detector modules.

## 2 DUNE

In an effort to measure oscillation probabilities for muon neutrinos or antineutrinos to either remain the same flavor or oscillate into their electron flavor counterparts, the international DUNE experiment is composed of three crucial components: a high-intensity neutrino beam produced by a proton accelerator, a near detector installed near the neutrino source, and finally a far detector placed at the end of the 1300km baseline which will be constructed 1.5km underground. The location and orientation of each of these components is summarized in figure (1).

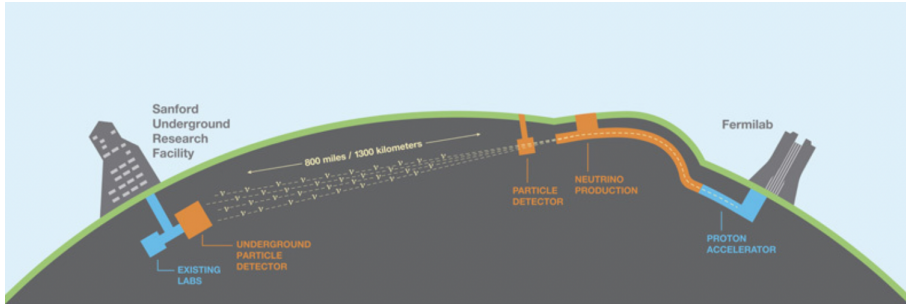


Figure 1: A schematic diagram describing the three main components of the DUNE physics program. Image taken from [1].

The far detector site will consist of four liquid argon time projection chamber modules which will be used to collect the vast majority of the data, and will be capable of reconstructing neutrino interactions with extremely high levels of resolution. Two of these modules will consist of single phase technology, while one of them will consist of dual phase technology; both of these methods are discussed in further detail in sections (2.3) and (2.4). Finally, the fourth module, the design of which has yet to be solidified, will consist of more advanced technology which is not discussed in this report. Conversely, the near detector will serve as the experiment's control, and will be used to measure initial, unoscillated neutrino energy spectrum. The near detector technology is discussed in further detail in section (2.2).

## 2.1 Goals

The central goals of the DUNE physics program are to further explore and understand the phenomenon of neutrino oscillations, discover implications that may lead to further solidification of grand unified theories, and to continue to test the validity of the standard models through the use of increasingly precise measurements and finer levels of precision.

Crutial attributes of the neutrino flavours and eigenstates remain unkown, most notably of which is the mass heirarchy. While there is current evidence of the ordering  $\nu_1, \nu_2, \nu_3$ , the reversed ordered holds reasonable precedence as well. Precise values of the mixing angles similarly remain uncertain. It is, however, known that  $\theta_{23}$  lie close to  $\pi/4$ , which maximizes the value of  $\sin \theta_{23}$ . Finally, the value of  $\delta_{CP}$  is minimally constrained – all values of  $\delta_{CP} \in [\pi, 2\pi]$  have supporting experimental evidence.

An alternative goal of the DUNE project is to be readily prepared for recording data from the burst of neutrinos emmited from core-collapses supernova events. In particular, the rarity of such events provides motivation for at least one detector to be active at all times to record such data. The core-collapse event is intialized with a brief and jagged burst of neutrinos, primarily composed of electron neutrinos. This is followed by a  $\sim 10$  second cooling phase, which holds the bulk of the potential information. The flavour content of the neutrino signal can then be in turn used to track the supernova's evolution.

## 2.2 Near Detector

One of the central goals of the DUNE physics program is to measure the oscillation probabilities for muon neutrinos  $\nu_\mu$  or their corresponding antineutrinos  $\bar{\nu}_\mu$  to either remain the same flavour, or to oscillate to the electron flavour  $\nu_e$  as a function of the neutrino energy. This will allow for concrete determination of the mass ordering, and enable potential observation of charge parity symmetry violations. The DUNE near detector will serve as the experiment's control, with it's central role being to measure the initial, unoscillated  $\nu_\mu$  and  $\nu_e$  energy spectra, as well as that of their corresponding antineutrinos. While doing so, the near detector will serve to minimize systematic error and uncertainty in the reconstruction of nucleon decay events.

In addition to being the experiment's control, the near detector will have its own physics program which will go beyond what the standard model has to offer. Namely, the near detector will search for non-standard interactions, sterile neutrinos, dark photons, and other exotic particle.

In summary, the DUNE near detector serves to measure initial neutrino energy spectra, predict the neutrino spectrum at the far detector site, measure neutrino interactions within the liquid argon to reduce nuclear modelling errors, and to monitor the neutrino beam. Perhaps the most important of these tasks is to compare the information of the events recorded at the far detector site to the predictions made at the near detector site based on differing sets of oscillation parameters. These parameters are subject to constraints from the data observed in the near detector.

## 2.3 Far Detector – Single Phase

In efforts to search for charge parity symmetry violations, observe and study nucleon decay, as well as potentially capture information of supernova collapses, it is essential that the DUNE detector be constructed using a large and stable reference mass. Due to the requirement that image reconstruction of such events have spatial resolution with a high level of accuracy, the far detector site will consist of two liquid argon time projection chamber modules using single phase technology, each containing at least 10 kilotons of liquid argon fiducial mass. These detectors will be installed 1500m underground, and will mark the end of the baseline of the experiment. The design of this module is summarized by figure 2 (left).

The defining property of the single phase technology is that *all* detector elements inside the chamber are immersed in liquid argon. The large volume of liquid argon is immersed within a strong electric field with strength of hundreds of volts per centimeter. As charged particles pass through this chamber, the liquid argon is ionized, causing the associated ionized electrons to drift horizontally within this electric field towards the anode plane wall, commonly referred to as an anode plane assembly array. This plane array consists of multiple layers of active wires directed in distinct directions, forming an electrically active grid. The voltage differences between these layers are chosen so that the drifting electrons are unimpeded by all but the final layer which collects the electrons, while the first layers produce induction signals which are read by the detector. An example of this technology is displayed by figure 2 (right).

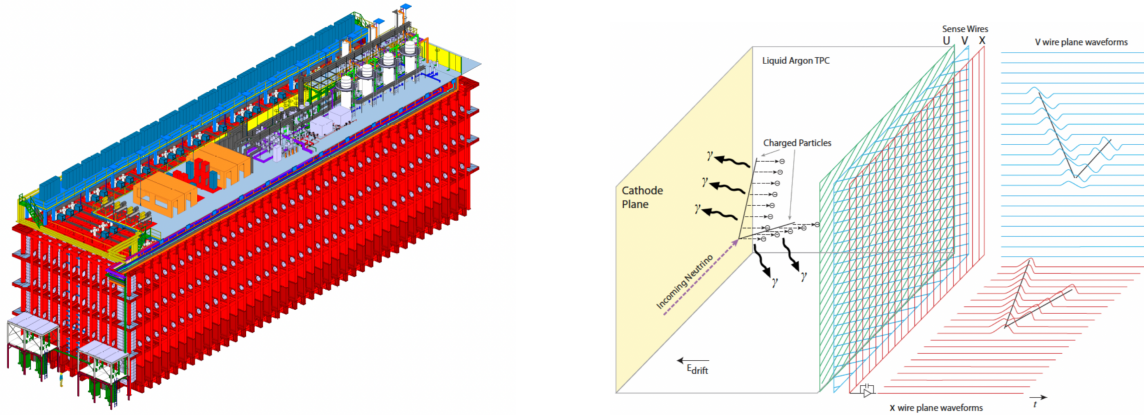


Figure 2: A schematic diagram displaying the entire single phase detector module that houses of 10kt fiducial liquid argon mass (left). A diagram displaying the construction of the anode plane assembly sense wires, and cathode plane orientation (right). Both of these images are taken from [1].

Once ionized, the liquid argon emits flashes of light vacuum ultraviolet light at a wavelength of 127nm. As the ultraviolet light crosses the detector, it is shifted to visible light which is in turn collected by the photon detectors. These detectors provide an initial propagation time  $t_0$ , which is then used in comparison with the time  $t_1$  at which the ionized electrons reach the anode plane to construct the exact state of the system [1]. This is a crucial step in calibrating the system to determine the precise properties of the nucleon-decay events and to apply drift corrections to the ionization charge.

The key component of the single phase far detector, however, is the patterns created by the ionized electrons along the anode plane assembly wall. The information collected from these patterns is essential to the reconstruction of the event in the coordinates perpendicular to the direction of propagation. The direction that the wires run in each layer of the anode planes are chosen as to optimize considerations of spatial resolution, but more importantly, optimize the signal-to-noise ratio of the ionization measurements [2]. Maximizing this ratio is crucial as recording ionization data is a measurement of the change in electric field with respect to position of the electrons, which directly enables the ability to identify distinct particles.

Maximizing the signal-to-noise ratio is a result of maximizing the purity of the liquid argon within the chamber. Achieving a purity level from electromagnetic contaminants of  $< 100$  parts per trillion leads to an ionized drift electron lifetime of over 3ms, which in turn ensures a signal-to-noise ratio greater than 5 for the induction planes, and greater than 10 for the collection planes [1].

## 2.4 Far Detector – Dual Phase

The potential to discover charge parity symmetry violations in the neutrino oscillation section, as well as observe and analyze nucleon decay and astrophysical events, is directly contingent on the detector's ability to obtain high

resolution images; the dual phase detector further augments this capability, relative to the single phase technology. In essence, these two modules operate in a very similar manor; charged particles that traverse the fiducial volume ionize the liquid argon, which in turn producing scintillation light which is accessible by the photon detectors.

In the dual space module, however, the resulting ionized electrons drift *vertically* in the liquid argon, and are eventually transferred to a layer of gaseous argon where the anode plane assembly resides. The collection, amplification, and measurement components of the dual phase detector are concatenated into layered modules, located at the top of the gaseous chamber, referred to as charge readout planes. The horizontally oriented charge readout plane consists of anode planes made from two double-sided printed circuit boards. The amplification component, essential to the maximization of the signal-to-charge ratio, consist of thin printed circuit boards, with a layer of electrodes placed on the top and bottom surfaces. Similar to the single phase technology, the charge readout plane also integrates a layer of immersed extraction grid, consisting of *xy*-oriented charged wires that provide the *xy* coordinates of an event.

The vertically oriented design of the dual phase module allows for a fully homogenous<sup>1</sup> liquid argon volume. This technology allows for increasingly long drift lengths, and ultimately reduces the quantity of nonactive materials in the chamber. Regardless of the longer drift lengths requiring a higher voltage of 600kV on the cathode, the dual phase design significantly improves the signal-to-noise ratio.

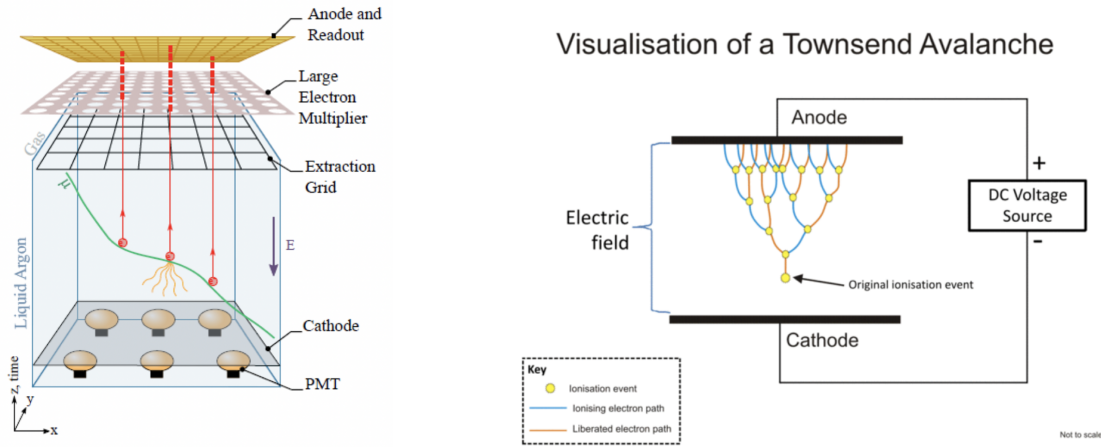


Figure 3: A diagram which labels the key components of the vertical drift chamber of the dual phase far detector module (left). A visualization of a Townsend Avalanche, particularly applicable to the technology included utilised in the far detector modules (right). The left image is taken from [1], and the right image is taken from [3].

The key differentiating component of the dual phase module with respect to the single phase module is the ability to implement charge amplification of the ionized signals. This is undergone through a process called 'avalanche'. The ionized electrons drift vertically through the time projection chamber until they reach the extraction grid which is situated just below to gas-liquid boundary. Once they reach this grid, the electrons are subjected to a stronger electric field in comparison to that of the drift field [2]. Once contained in the gaseous chamber, the electrons interact with large electron multiplier detectors which are encoded with a micro-pattern of high-field regions– regions which greatly amplify the electron signals.

The amplification process is underwent via avalanches caused by Townsend multiplication, a process which operates under three major steps which are summarized by the schematic diagram in figure 3. The process begins with an initiation phase which is activated by the presence of an initial charged particle within the gaseous chamber. This electron gains energy and accelerates due to an electric field applied across the gas. The initiation phase is followed by the collision phase, in which the accelerated electron collides with gas molecules. During these collisions, the electron transfers some of its energy to the gas molecules, ionizing them by knocking out electrons from the gas molecules. This step is followed by the electron multiplication in which the newly created electrons roam free within the gas, and are in turn also accelerated by the electric field. These secondary electrons, created in the ionization process, initiate further ionization events by colliding with other gas molecules. This process results in the exponential growth in the number of charged particles within the gaseous projection chamber [5]. The use of avalanches to amplify the signal produces by the charges in the gaseous chamber increases the signal-to-noise ratio by a predicted factor of 10, which will significantly improve the event reconstruction quality, in comparison to the single phase technology [1].

<sup>1</sup>The word 'homogenous', in this case, refers to the uniformity and consistency of the liquid argon volume; There are no variations or distinct regions within the liquid argon volume that have different characteristics

## References

- [1] B. Abi et al. “Volume I. Introduction to DUNE”. In: *JINST 15 T08008* (2020).
- [2] B. Abi et al. “Volume III. Introduction to DUNE”. In: *JINST 15 T08009* (2020).
- [3] DougSim. “Townsend discharge”. In: *Wikipedia* (2021).
- [4] Francesco Terranova Mauro Mezzetto. “Three-flavour oscillations with accelerator neutrino beams”. In: *Multidisciplinary Digital Publishing Institute* (2020).
- [5] Yuri P. Raizer. “Gas Discharge Physics”. In: *Springer* (1991).